International Journal of Solids and Structures 49 (2012) 2934–2940

Contents lists available at SciVerse ScienceDirect

International Journal of Solids and Structures

journal homepage: www.elsevier.com/locate/ijsolstr

Influence of temperature on a carbon–fibre epoxy composite subjected to static and fatigue loading under mode-I delamination

P. Coronado [a], A. Argüelles [a], J. Viña [a,*], V. Mollón [b], I. Viña [b]

[a] Department of Construction and Manufacturing Engineering, University of Oviedo, 33203 Gijón, Spain
[b] Department of Materials Science and Metallurgical Engineering, University of Oviedo, 33203 Gijón, Spain

ARTICLE INFO

Article history:
Received 27 December 2011
Received in revised form 17 May 2012
Available online 12 June 2012

Keywords:
Mode I
Temperature
Fatigue
Fracture

ABSTRACT

In this paper, interlaminar crack initiation and propagation under mode-I with static and fatigue loading of a composite material are experimentally assessed for different test temperatures. The material under study is made of a 3501-6 epoxy matrix reinforced with AS4 unidirectional carbon fibres, with a symmetric laminate configuration $[0°]_{16/S}$. In the experimental programme, DCB specimens were tested under static and fatigue loading. Based on the results obtained from static tests, fatigue tests were programmed to analyse the mode-I fatigue behaviour, so the necessary number of cycles was calculated for initiation and propagation of the crack at the different temperatures. G–N curves were determined under fatigue loading, N being the number of cycles at which delamination begins for a given energy release rate. G_{ICmax}–a, a–N and da/dN–a curves were also determined for different G_{cr} rates (90%, 85%, 75%, etc.) and different test temperatures: 90 °C, 50 °C, 20 °C, 0 °C, −30 °C and −60 °C.

1. Introduction

Fibre-reinforced composites represent an evolution with respect to traditional materials due to the benefits provided by their orthotropic structure, which enables the fibres to guide the direction in which stresses act. As carbon–fibre epoxy composites offer the best mechanical properties with low weight, they are commonly used in aerospace and naval applications, competitive sports and high technology applications in general. However, despite their specific strength and stiffness, one of the most life-limiting failure modes in these materials is the phenomenon known as delamination due to the fact that they are composed of laminated layers.

The fracture mechanics of these materials under static and fatigue loading are currently the subject of extensive study as these mechanisms have yet to be adequately explained as a result of their complexity.

In recent years, several studies have been carried out into the fracture of composites in their different stress modes under static loading, of which modes I and II have attracted more attention. The dynamic fracture regime is different because it has been under-researched on account of the difficulties associated with experimentation (Anderson et al., 2004; Argüelles et al., 2008; Shivakumar et al., 2005; Turon et al., 2007). The relationship between the static and fatigue strength of composites and the temperature is of crucial importance for the design of structures made with these materials. Nonetheless, few studies have been carried out to date (Asp, 1998; Sjögren and Asp, 2002) due to the complexity of the tests, the number of papers analysing the behaviour of composites at low temperatures still being substantially low (Kalarikkal et al., 2006; Shindo et al., 2006; Sumikawa et al., 2005). The main objective of this paper is to analyse the process of delamination of a carbon/epoxy composite when is subjected to temperatures equivalent to those that occur in service in different applications mainly aeronautics. For this, an experimental programme, where the specimens were tested both statically and fatigue under mode I, was performed at different operating temperatures: −60, −30, 0, 20 (room temperature), 50 and 90 °C, determining the influence of temperature on the toughness (G_{IC}) values obtained.

2. Experimental procedure

2.1. Materials and specimens

The composite material employed in this research programme was manufactured by Hexcel Composites and is composed of a 3501-6 epoxy resin prepreg reinforced with AS4 unidirectional carbon fibre (commercially named AS4/3501-6 RC37 AW190). The cured panels are obtained by cutting prepreg laminates, sequentially piled and cured in autoclave, with a volume fraction of 63%. The laminate configuration is symmetric $[0°]_{16/S}$, employing

* Corresponding author. Tel.: +34 985182021; fax: +34 985182022.
E-mail address: jaure@uniovi.es (J. Viña).

0020-7683/$ - see front matter
http://dx.doi.org/10.1016/j.ijsolstr.2012.05.018

a 10 μm thick Tygavac RF-242 film at the midplane, as insert to form an initiation site for the delamination.

A double cantilever beam (DCB) specimen was used to characterise delamination under mode-I conditions for both static and fatigue loading. Fig. 1 shows the geometry of the specimen according to the Standard (ASTM D5528-01, 2001). The dimensions of the specimens used were: L = 200 mm, B (specimen width) = 25 mm, h = 6 mm and a_0 = 50 mm.

2.2. Test procedure

Prior to testing, the specimens were conditioned as indicated by the Standards (ASTM D5528-01, 2001; ASTM D6115-97, 1997) for static and fatigue tests, respectively. All the tests were carried out on a servo-hydraulic MTS testing machine provided with a 1kN load cell controlled by a computer using the original software. A thermal chamber was coupled to the testing machine to carry out the high temperature tests (50 and 90 °C). For the low temperature tests (0, −30 and −60 °C), the same thermal chamber was used with a liquid nitrogen bottle attached to it. In order to facilitate visual monitoring of the progress of delamination, one of the edges of the specimens was covered with white paint spray and graduation marks each millimetre were performed. A TV camera (Pulinex model TM-7CN which use a 1/2 in. high resolution imager and ×100 zoom) focused on the graduated edge and connected to a monitor was used to observe the advance of the crack. This solution was necessary because it was not possible in the tests carried out inside the thermal chamber to observe the crack growth with a microscope as shown in the standard.

In this study, instead of attaching the specimens to the grips by means of adhesive blocks or hinges as specified in the Standard, a 15 mm deep and 2 mm thick notch was made on the film area of the specimen and mechanical grips were employed similar to those used by Blanco et al. (2008), but modified by Viña et al. (2012), in their study of the delamination of composite laminates in mixed mode and similar to that used by Brandt in a previous work (Brandt, 1998), Fig. 2. The purpose of this modification in the test was to avoid problems with the detaching of the hinges or blocks due to failure of the adhesive during the tests at high and low temperatures. In addition, an extensometer (MTS, 12.5 mm) was coupled to the area of the insert of the specimen to obtain data on the opening of the lips of the crack and to relate such data to the readings of the visual measures of crack growth, thus enabling automated fatigue testing based on previous static tests.

Specimens should not be precracked before testing. The static tests were carried out using a constant crosshead rate of 1 mm/min for initiation and 0.5 mm/min for reloading.

To characterise the behaviour under fatigue of the material, DCB specimens were cycled between a maximum and minimum displacement (δ_{max} and δ_{min}) that varied depending on crack growth. The values of the opening of the crack front provided by the extensometer measurements (ΔL) were accordingly related to the visual measurements of the progress of delamination (a) in the static

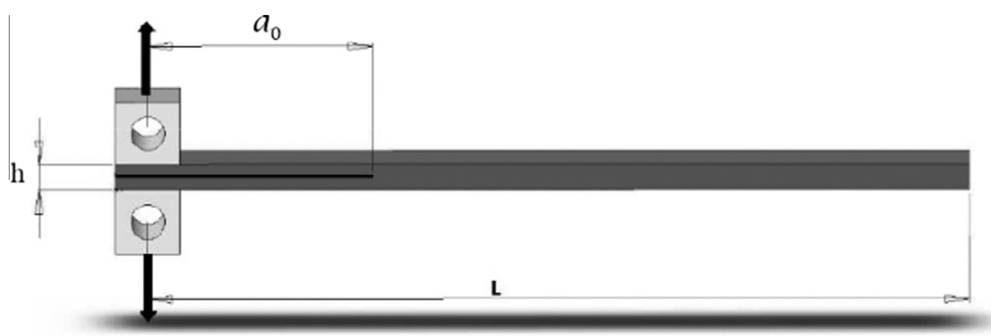

Fig. 1. DCB specimen geometry (double cantilever beam).

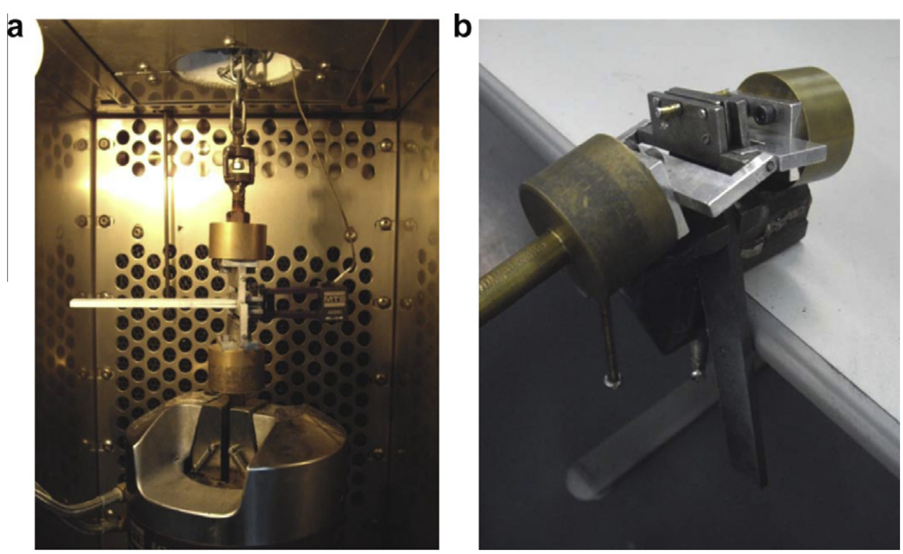

Fig. 2. Test procedure: (a) specimen with the extensometer inside thermal chamber and (b) specimen with mechanical grips.

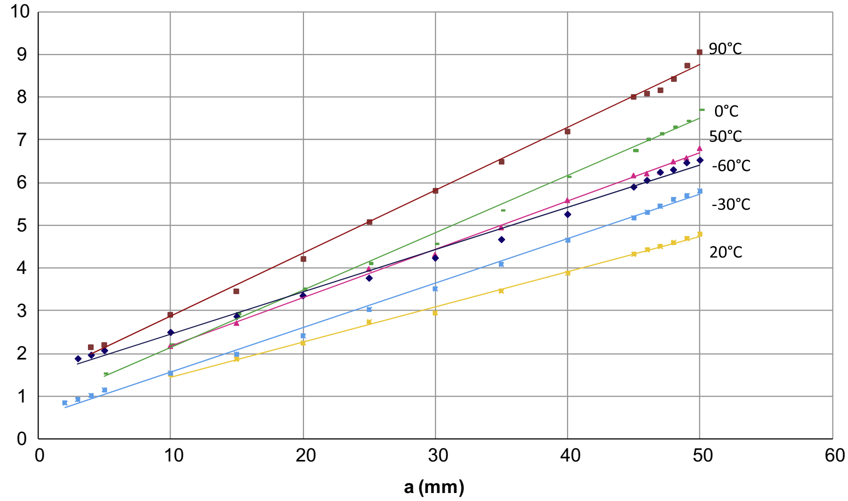

Fig. 3. Extensometer readings based on the progress of the delamination of the most representative specimens in the static tests.

tests. As can be seen in Fig. 3, this relationship is linear for all the analysed temperatures. Thus, the position of delamination can be predicted in accordance with the measurements obtained by the extensometer.

A test procedure was created on the test machine for each temperature and the different fractions of the critical energy release rates G_{crit} (65%, 75%, 85%, etc.) in order to automate the tests, in which each part of the test varied depending on the length of the crack, obtained directly from the extensometer. This procedure enables us to determine and record the position of the crack during the fatigue tests and the level of load provided that the fracture energy applied to the specimen remains constant throughout the test. A frequency of 3 Hz and asymmetry coefficient $R = 0.2$ were applied in the fatigue tests.

3. Experimental results

The experimental results obtained from the static and fatigue tests for the thermal analysis for the material AS4/3501-6 are presented next.

3.1. Static delamination

The initial part of the test consisted in increasing the crack length from 3 to 5 mm, loading the specimens at a constant crosshead rate of 1 mm/min. Five specimens were tested for each temperature. Fig. 4 shows the load–displacement average curves for each temperature, being the displacement the axial movement of the actuator of the testing machine. Also, the slope for each line has been calculated. It can be observed a slight loss in bending stiffness in the specimens tested at the extreme temperatures (90 and −60 °C), where the slopes get less than the other temperatures analysed.

Interlaminar fracture toughness in mode-I was calculated for a better characterisation of the mechanical properties of the material. The test results were evaluated using three data reduction methods for calculating the interlaminar fracture toughness (G_{IC}) as recommended in the Standard: MBT (Modified Beam Theory Method), CC (Compliance Calibration Method) and MCC (Modified Compliance Calibration Method). The MBT was chosen to present the results on account of being the most conservative method. Table 1 shows the mean values of the interlaminar fracture tough-

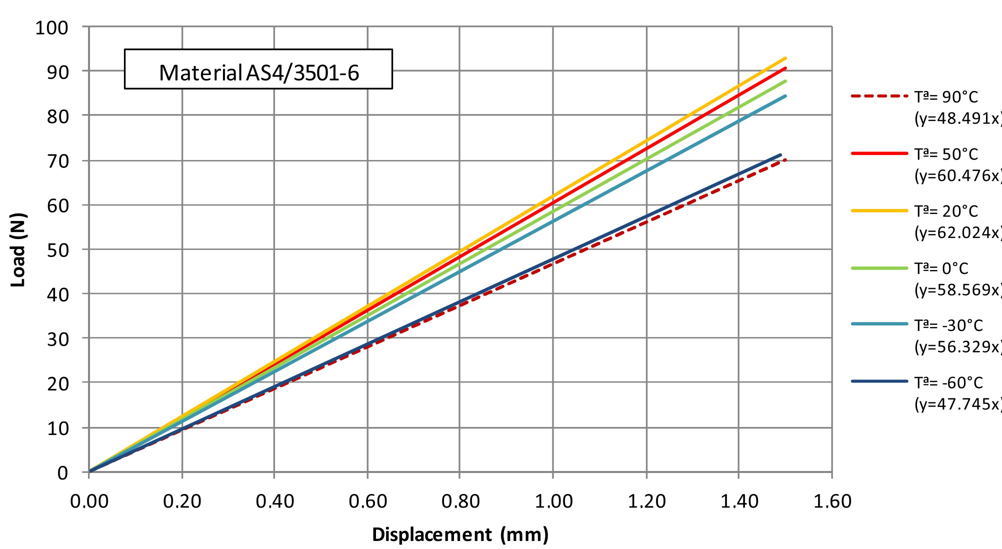

Fig. 4. Load and displacement values during static initiation of the crack for AS4/3501-6 for each test temperature.

Table 1
Mean values of G_{IC} during the initiation of static delamination.

G_{IC} (AS4/3501-6)	T^a = 90 °C	T^a = 50 °C	T^a = 20 °C	T^a = 0 °C	T^a = −30 °C	T^a = −60 °C
MBT [J/m^2]	165.62	151.94	129.79	89.68	105.00	110.39
CC [J/m^2]	192.70	169.32	131.51	91.30	111.59	114.77
MCC [J/m^2]	170.87	150.23	128.71	88.54	107.90	114.88
Mean	176.40	157.16	130.01	89.84	108.16	113.35
Coefficient variation [%]	8.14	6.72	1.08	1.55	3.05	2.26

ness (G_{IC}) obtained from the three methods with the variation in the results versus temperature. As this table shows, the highest values of G_{IC} were obtained at high temperature tests.

A constant crosshead rate of 0.5 mm/min was applied in the reloading process for static crack growth in order to ensure effective chase of the crack tip. In order to analyse the static propagation of delamination, the values of G_{IC} were represented as a function of the crack length of the most representative specimens for each temperature in Fig. 5. The graph shows an increasing trend in toughness values with increasing crack length, probably due to fibre bridging. The material under study presented a higher toughness during the tests performed at 90 °C.

3.2. Fatigue delamination

In order to characterise the initiation process of delamination due to fatigue, the number of cycles required to generate a crack in the material were determined by direct observation of the specimen. This process was characterised by the G_{ICmax}–N curve, Fig. 6, which graphically defines the number of cycles required to initiate

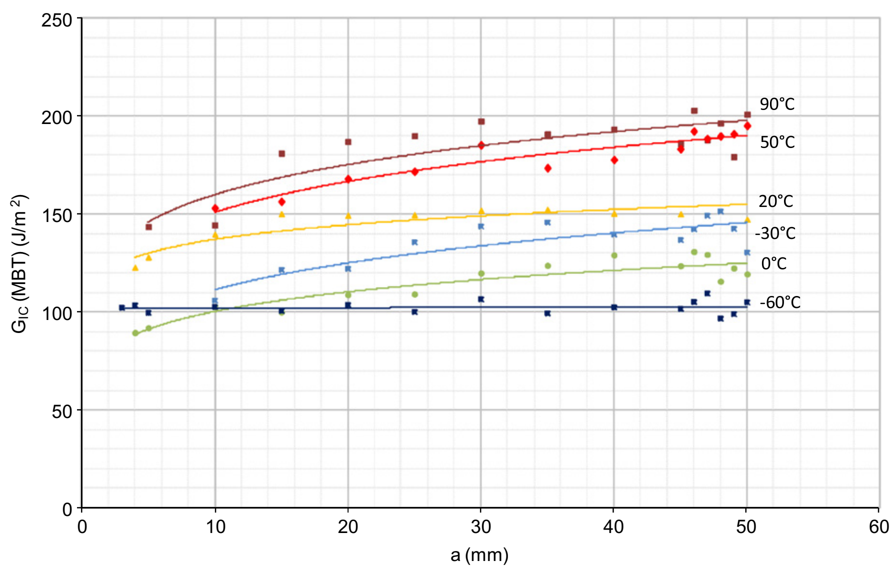

Fig. 5. G_{IC} values (MBT) versus the advance of delamination obtained from the most representative specimens for each test temperature.

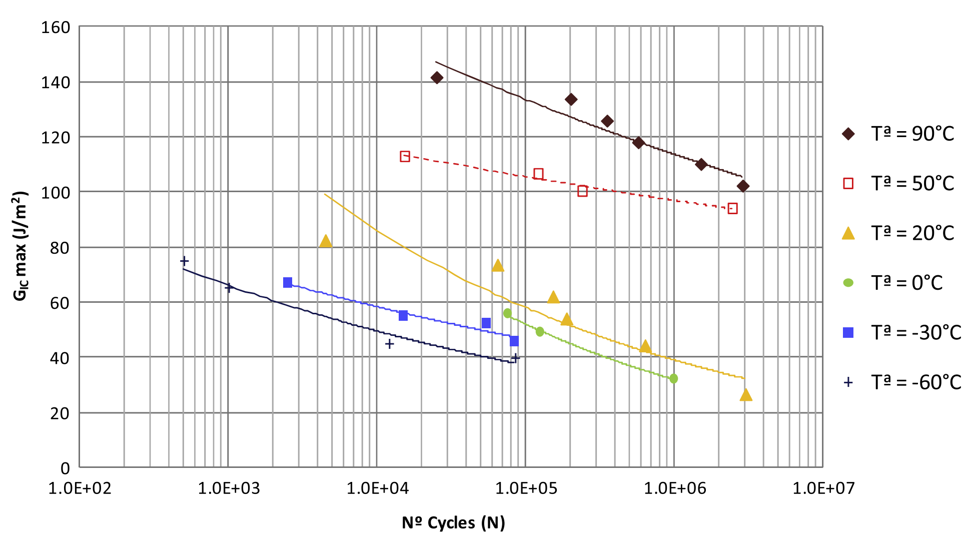

Fig. 6. Initiation curve of delamination by fatigue for the composite AS4/3501-6 at the different test temperatures.

the crack in terms of the maximum delamination energy used (G_{ICmax}) for different test temperatures. The plot shows how the G_{ICmax} needed to initiate delamination increases with increasing temperature and decreases progressively when the number of cycles increases after crack initiation.

The crack growth rate (da/dN) versus delamination length (a) at an energy level of 75% G_{max} (obtained in static tests) for the entire temperature range studied was used to analyse the velocity of fatigue propagation of the AS4/3501-6, in Fig. 7. The results show a constant crack growth rate while delamination advances, except for the tests performed at low temperatures (−30 and −60 °C), where the speed of propagation is initially quite high and then decreases as the crack spreads.

Fig. 8 shows the G_{ICmax}–a curve, which graphically defines crack growth (a) as a function of the maximum delamination energy used (G_{ICmax}) at an energy level of 75% of G_{max} (obtained from static tests) during the dynamic propagation process for all the temperatures studied. The graph shows that in order to achieve the same crack length, the maximum fracture energy needed is greater for tests performed at 90 °C. Furthermore, as with the tests performed at room temperature, the fracture energy increases as delamination progresses.

Fig. 9 shows the progression of delamination versus the number of cycles, i.e. the a–N curves. The graph shows that in order to reach the same crack length, the number of cycles required is greater in tests at 20, 50 and 90 °C due to more ductile behaviour of the matrix.

4. Fracture surfaces analysis

A fractographic study was performed using a scanning electron microscope (SEM) on samples obtained from the previously tested specimens in mode-I static and fatigue fracture, Fig. 10, in order to analyse the fracture surfaces at the different test temperatures.

The micrographs thus obtained show different morphologies typical of mode-I fracture. In general, under mode I loading the fibres were separated by fairly flat-sided valleys (Singh and Greenhalgh, 1997), and the so-called "river markings" (Smith and Grove, 1987) were generally observed, which indicate a plastic behaviour of the matrix (Mollón et al., 2012). As the temperature decreases these markings gradually give way to a brittle aspect of the matrix. In tests at high temperatures, an increase in the ductility of the matrix can be observed with increasing temperature, a feature that is appreciated by the deformation observed in the matrix itself and the amount of resin adhered to the fibres on the fracture surfaces of the tested specimens. Areas where the matrix developed a higher degree of deformation were observed in the fractographic analysis as shows Fig. 10e. This photograph shows the sporadic "lamelle structure" or "hackle pattern" generated by

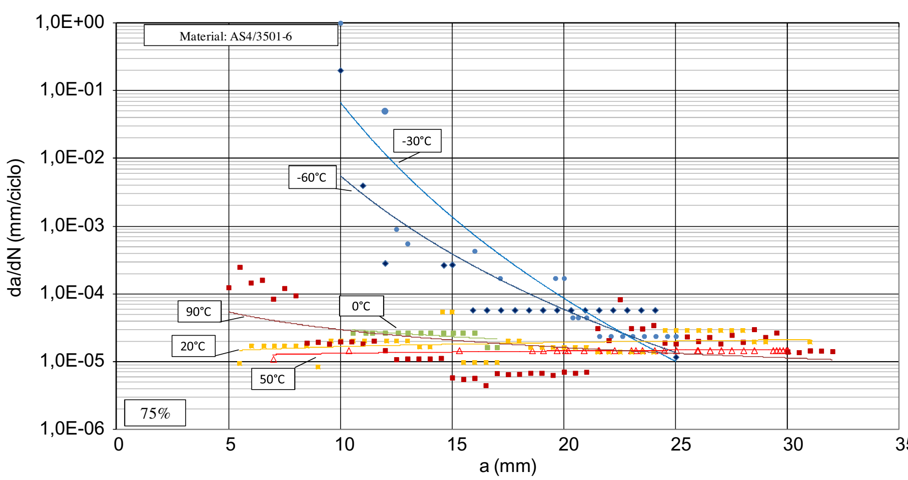

Fig. 7. Crack growth rate (da/dN) versus crack length (a) of the material AS4/3501-6 for each analysed temperature: 90, 50, 20, 0, −30 and −60 °C.

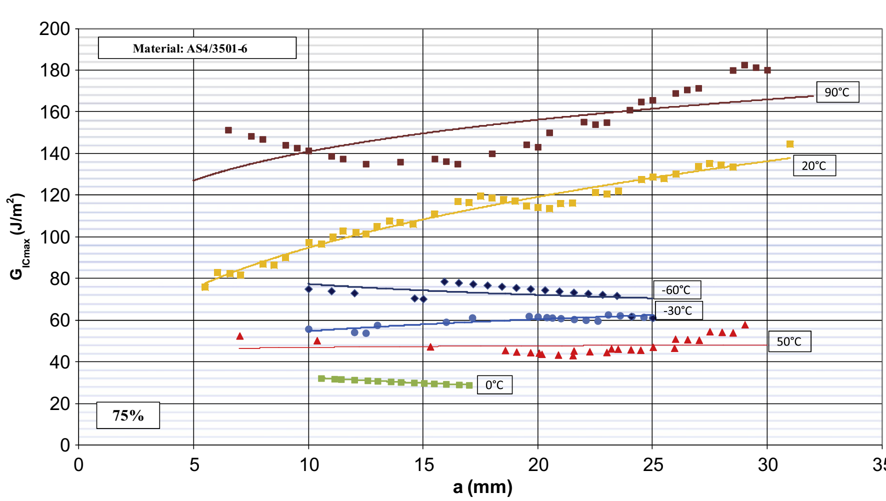

Fig. 8. Maximum delamination energy (G_{ICmax}) versus crack length during the dynamic propagation procedure for each analysed temperature.

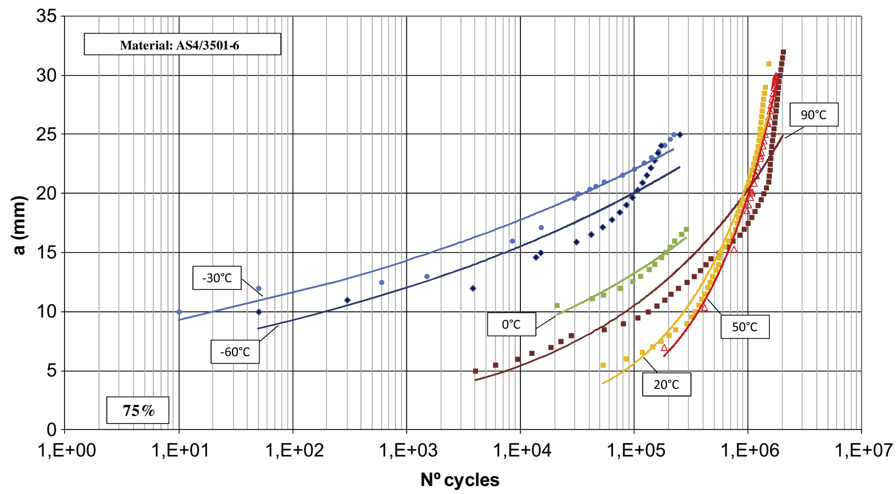

Fig. 9. Advance of delamination based on the number of cycles for an energy level of 75% G_{max} (obtained in static tests) for all the test temperatures.

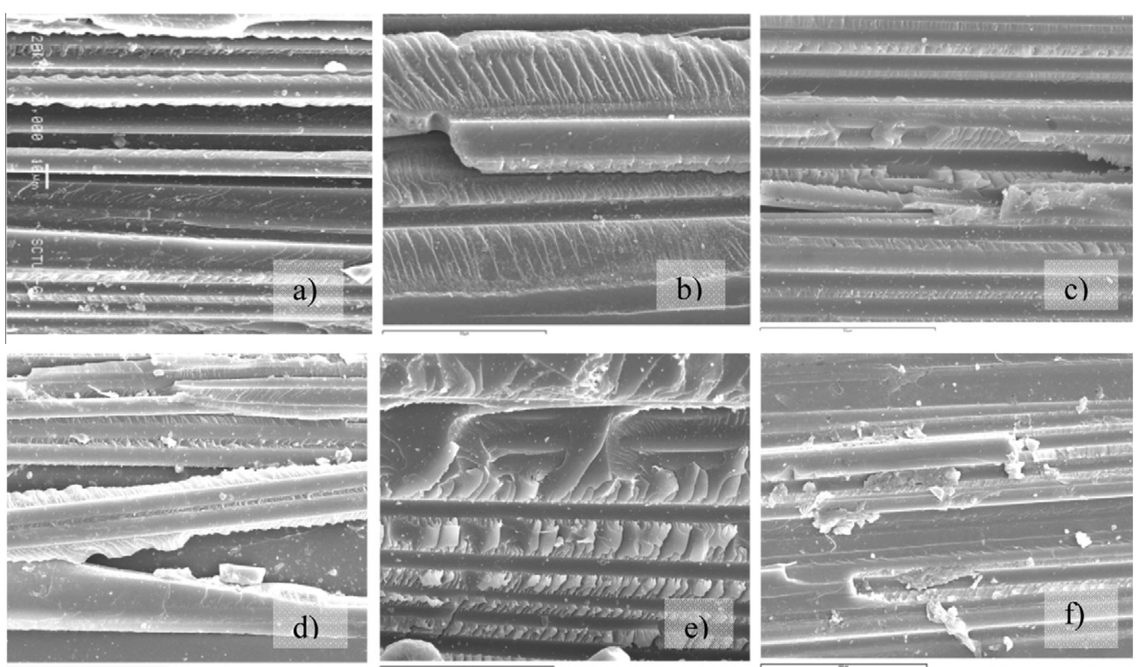

Fig. 10. Fracture surface of fatigue tested AS4/3501 specimens: (a) 20 °C, (b) 50 °C, (c) 90 °C (d) 0 °C, (e) −30 °C and (f) −60 °C (×1000).

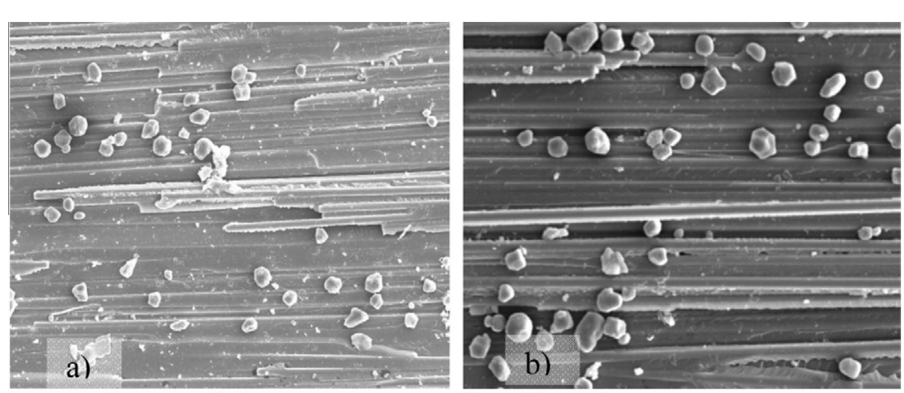

Fig. 11. AS4/3501-6 fatigue tested at: (a) −60 °C (×250) and (b) −30 °C(×350).

a mixed mode loading condition as have reported some authors in mode I, mode II and mixed modes (Roulin-Moloney, 1989). This pattern was observed in local regions and can appear due to fibre bridging. At temperatures of 0, −30 and −60 °C, small spherical portions of matrix can be observed. These were analysed to confirm that this was not dirt, Fig. 11, resulting from the brittle behaviour of the matrix at low temperature tests.

Another general morphology at all the test temperatures comprises the voids in the fibres, which were generally clean, indicating a progression of delamination in the fibre–matrix interface. Broken fibres were also found in the micrographs resulting from "fibre bridging", one of the characteristic morphologies of mode-I fracture.

5. Conclusions

This paper has analysed the influence of temperature on the process of mode-I delamination in a carbon fibre reinforced epoxy material under static and fatigue loadings.

– In the studies carried out to characterise the static initiation of delamination, in general, a slight decrease in stiffness was observed for the highest and the lowest temperature. However, the material exhibits better mechanical behaviour in the tests performed at 9 °C in the static initiation phase, where obtained the highest values of G_{IIC} due to a slight increase in ductility in the matrix. When the test temperature decreases, less fracture energy is required to initiate the delamination.
– As to static delamination propagation, a general increasing trend in toughness (G_{IC}) was observed as delamination progressed, due to fibre bridging, thereby increasing the resistance to delamination of the material.
– During the initiation of fatigue delamination, it was observed that the maximum delamination energy required to initiate the crack (G_{ICmax}) increased with increasing test temperature and decreased significantly after initiation of the crack with the increasing number of cycles.
– A constant delamination growth rate (da/dN) was observed in the fatigue propagation of the crack, except for tests under the most extremely cold conditions (−30 and −60 °C), where the growth rate was significantly higher, decreasing as the crack progressed, thus indicating a more brittle behaviour of the matrix.
– As it was observed with the static propagation of delamination, in the tests performed at 90 °C, the highest values of G_{ICmax} were obtained during fatigue propagation due to the more ductile behaviour of the matrix with increasing test temperatures.
– In general, the behaviour of AS4/3501-6 was influenced by the test temperature, although this fact is most noticeable in the fatigue tests, probably due to the length of the tests. In general, the analysed composite shows more brittle behaviour at low temperatures and a significant increase in the ductility of the matrix as the temperature increases. During static tests, the material performs better at room temperature. During fatigue tests, however, the ductility of the matrix increases at 90 °C, leading to greater resistance to delamination during the dynamic propagation procedure.
– As regards the fractographic analysis of the fracture surfaces, it may be concluded that, in addition to the observed typical morphologies of mode-I fracture, the analysed micrographs have a relationship with the results obtained during the experimental procedure.

Acknowledgements

The authors are indebted to the Spanish Ministry of Science and Innovation (Project MAT2010-14943) for partial funding of this work.

References

Anderson, J., Hojo, M., Ochiai, S., 2004. Empirical model for stress ratio effect on fatigue delamination growth rate in composite laminates. Int. J. Fatigue 26, 597–604.
Argüelles, A., Viña, J.F., Canteli, A., Castrillo, M.A., Bonhomme, J., 2008. Interlaminar crack initiation and growth rate in a carbon–fibre epoxy composite under mode-I fatigue loading. Compos. Sci. Technol. 68, 2325–2331.
Asp, L.E., 1998. The effects of moisture and temperature on the interlaminar delamination toughness of a carbon/epoxy composite. Compos. Sci. Technol. 58, 967–977.
ASTM D5528-01, 2001. Standard test method for mode I interlaminar fracture toughness of unidirectional fiber–reinforced polymer matrix composites.
ASTM D6115-97, 1997. Standard test method for mode I fatigue delamination growth onset of unidirectional fiber–reinforced polymer matrix composites.
Blanco, N., Gamstedt, E.K., Costa, J., 2008. Mechanical hinge system for delamination tests in beam-type composite specimens. Compos Sci. Technol. 68, 1837–1842.
Brandt, F., 1998. New load introduction concept for improved and simplified delamination beam testing. Exp. Tech. 22 (1), 17–20.
Kalarikkal, S.G., Sankar, B.V., Ifju, P.G., 2006. Effect of cryogenic temperature on the fracture toughness of graphite/epoxy composites. J. Eng. Mater. Technol. – Trans ASME 128, 151–157.
Mollón, V., Bonhomme, J., Viña, J., Argüelles, A., Canteli, A.F., 2012. Influence of the principal stresses on delamination fracture mechanisms and associated morfology for different loading modes in carbon/epoxy composites. Composites Part B 43, 1676–1680.
Roulin-Moloney, A.C., 1989. Fractography and Failure Mechanism of Polymers and Composites. Elsevier Applied Science.
Shindo, Y., Inamoto, A., Narita, F., Horiguchi, K., 2006. Mode I fatigue delamination growth in Gfrp woven laminates at low temperatures. Eng. Fract. Mech. 73, 2080–2090.
Shivakumar, K., Chen, H., Abali, F., Le, D., Davis, C., 2005. A total fatigue life model for mode I delaminated composite laminates. Int. J. Fatigue 28, 33–42.
Sjögren, A., Asp, L.E., 2002. Effects of temperature on delamination growth in a carbon/epoxy composite under fatigue loading. Int. J. Fatigue 24, 179–184.
Smith, B.W., Grove, R.A., 1987. ASTM STP 948, pp. 154–173.
Sumikawa, M., Shindo, Y., Takeda, T., Narita, F., Takano, S., Sanda, K., 2005. Analysis of mode I interlaminar fracture and damage behavior of Gfrp woven laminates at cryogenic temperatures. J. Compos. Mater. 39, 2053–2066.
Singh S., Greenhalgh E.S., 1997. Micromechanisms of interlaminar fracture in carbon-epoxy composites at mulridirecctional ply interfaces. In: 4th International Conference on Deformation and Fracture of Composites, pp. 201–210.
Turon, A., Costa, J., Camanho, P.P., Davila, C.G., 2007. Simulation of delamination in composites under high cycle fatigue. Compos. Part A – Appl. Sci. Manuf. 38, 2270–2282.
Viña, J., Argüelles, A., López, A., Mollón, V., Bonhomme, J., 2012. Influence of the loading system on mode I delamination results in carbon–epoxy composites. Exp. Tech. http://dx.doi.org/10.1111/j.1747-1567.2011.00793.x.